Polariton light-emitting diode in a GaAs-based microcavity

Daniele Bajoni,[1] Elizaveta Semenova,[1] Aristide Lemaître,[1] Sophie Bouchoule,[1] Esther Wertz,[1] Pascale Senellart,[1] and Jacqueline Bloch[1,*]

[1]*CNRS-Laboratoire de Photonique et de Nanostructures, Route de Nozay, 91460 Marcoussis, France*

(Received 11 January 2008; published 5 March 2008)

Cavity polaritons have been shown these last years to exhibit a rich variety of nonlinear behaviors which could be used in new polariton based devices. Operation in the strong coupling regime under electrical injection remains a key step toward a practical polariton device. We report here on the realization of a polariton based light-emitting diode using a GaAs microcavity with doped Bragg mirrors. Both photocurrent and electroluminescence spectra are governed by cavity polaritons up to 100 K.

DOI: 10.1103/PhysRevB.77.113303 PACS number(s): 73.50.Pz, 78.55.Cr, 78.60.Fi, 71.36.+c

As first predicted by Purcell in 1946,[1] spontaneous emission of light can be strongly modified when inserting an emitter in a resonant cavity. When the emitter is located at an antinode of the electromagnetic field, the emission of light can be strongly accelerated or even become reversible if the light-matter coupling is strong enough. In such strong coupling regime, the degeneracy between the emitter and the photon mode is lifted giving rise to two light-matter entangled eigenstates spectrally separated by the Rabi splitting. This strong coupling regime has been first evidenced for atoms in ultrahigh finesse microcavities[2] and more recently in various solid state systems such as a superconducting q-bit,[3] quantum well excitons in inorganic[4] or organic semiconductors,[5] intersubband transition in two dimensional electron gas,[6] or excitons in single quantum dots.[7–9] Cavity polaritons, resulting from the strong coupling regime between excitons in quantum wells and cavity photons, have been the subject of intensive research since their discovery in 1992.[4] In two dimensional cavities, each exciton with a given in-plane wave vector $k_{\|}$ is coupled to the photon mode with the same $k_{\|}$. The strong coupling regime gives rise to two polariton branches with a pronounced energy trap of the lower branch close to $k_{\|}=0$.[10] The bosonic nature of polaritons in addition to the strong polariton-polariton interactions are responsible for a rich variety of nonlinear behaviors in inorganic materials: polariton accumulation in the ground state and formation of a macroscopically occupied coherent state,[11–15] photon pair emission,[16] or spin current generation.[17] These features are promising for future quantum applications but have up to now only been observed under optical pumping. Electrical injection of these entangled light-matter states is a key step toward the implementation of practical, compact devices. So far, electrical injection of cavity polaritons has been reported in organic semiconductors[18] where the coupling strength is very large (Rabi splitting of several hundreds of meV). More recently, electrical injection of polaritons using intersubband transitions in GaAs have been reported.[19] However, to our knowledge, nonlinearities have not been observed using either of these schemes. The GaAs system, when relying on interband transitions, is very attractive since its strong nonlinearities could be exploited in an electrically pumped device.

In the present Brief Report, we report on the realization of a GaAs microcavity containing quantum wells and surrounded by two doped Bragg mirrors. Both photocurrent spectra and electroluminescence evidence two well-resolved polariton branches up to 100 K. Increasing the current density, electroluminescence spectra reveal the progressive transition from the strong coupling regime to the weak coupling regime because of exciton screening at high carrier density. These findings open the way toward future polariton based devices.

The cavity structure is shown in Fig. 1(a): It consists in an undoped GaAs cavity containing three $In_{0.05}Ga_{0.95}As$ quantum wells and surrounded by two $Ga_{0.9}Al_{0.1}As/Ga_{0.1}Al_{0.9}As$ Bragg mirrors. The mirrors are doped to inject or collect carriers into or from the active region. The cavity layer is undoped so that the excitonic character of the quantum well

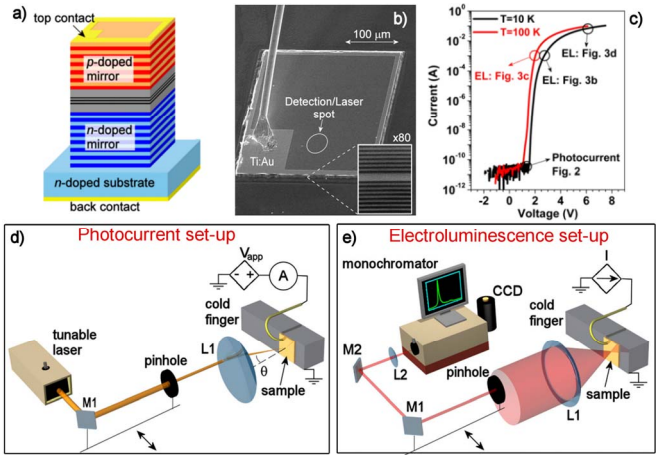

FIG. 1. (Color online) (a) Schematic view of the sample structure. (b) Scanning electronic microscope image of a mesa showing the lateral contact and the top injection wire. Also indicated is the typical size of the optical excitation and/or detection spot. In the inset a magnified image of the mesa edge reveals the multilayer structure with the cavity in the middle. (c) Current-voltage characteristics measured at 10 and 100 K. The circles indicate the operating conditions used in the experiments described in this Brief Report. (d) Schematic view of the setup for photocurrent measurements: the sample is excited with a tunable laser controlling both the energy and the angle of incidence of the exciting beam while the induced current is detected. (e) Schematic view of the setup for electroluminescence measurements: a current is injected through the sample and the induced emission is monitored for various detection angles.

emission is preserved. The sample was grown by molecular beam epitaxy on an n-doped GaAs substrate. The top (bottom) mirror is p-doped (n-doped) and contains 20 (24) pairs. The p-doped Bragg mirror is completed by a highly doped $p++$GaAs thin top contact layer. Al graded concentrations at each interface in the Bragg mirror are introduced to optimize mirror resistance. The structure is designed so that the quantum well exciton emission is close to resonance with the cavity mode at low temperature. A slight wedge of the cavity layer allows fine tuning of the cavity mode.

Square mesas of 300 μm lateral size were etched down to the GaAs substrate using optical lithography and wet chemical etching. Ti-Au was evaporated to form the top lateral p-type contact and was completed in the inside by a semitransparent (40% transmission) Au layer to ensure uniform electrical injection over the entire diode surface. AuGeNi was evaporated and alloyed on the backside of the wafer to form the bottom n-type contact. Such mesas were defined at different positions of the wafer, corresponding to different detunings between the cavity mode and the quantum well energy.

The sample is kept at low temperature in a cold finger cryostat. For photocurrent measurements [Fig. 1(d)], the sample is biased with a stabilized voltage source. A cw Ti-:sapphire laser beam is focused on the sample (50 μm diameter spot) with a 50 mm focal lens (L1). The excitation incident angle is controlled by a pinhole placed close to the Fourier plane of L1 (1° angular resolution). For electroluminescence measurements [Fig. 1(e)], the inverse scheme is used. The sample is driven by a stabilized current source. The emission is collected through L1 and through the pinhole and analyzed with a monochromator followed by a nitrogen cooled Si charge coupled device camera.

The electrical characteristics of the device at 10 and 100 K are shown in Fig. 1(c). A typical diodelike behavior is evidenced with a band alignment around 1.5 V. Below 1.5 V, the built-in electric field prevents forward current from flowing through the structure. Because of the low operating temperature, reverse current is not detectable. Under optical excitation, photogenerated carriers flow from the quantum well toward the contacts (electrons into the n contact and holes into the p contact), thus generating a reverse photocurrent. On the other hand, when a voltage above 1.5 V is applied, a forward current is generated through the structure: electrons and holes recombine in the undoped region giving rise to an electroluminescence signal. Both operating conditions are described below.

Let us first consider the reverse bias regime[20] where a voltage of 1.3 V is applied to the photodiode at 10 K. The photocurrent spectra shown in Fig. 2(a) were measured by optically exciting the sample at various incident angles. Two dips are evidenced in each photocurrent spectrum. For a given incident angle, the laser selectively excites polariton states with $k_{\parallel}=E(k_{\parallel})\sin(\theta)/\hbar c$, where $E(k_{\parallel})$ is the polariton energy. Thus, these photocurrent measurements directly map the polariton dispersion by probing the absorption. The energy of the photocurrent dips is summarized in Fig. 2(b) as a function of θ: Two polariton branches are observed presenting the anticrossing characteristic of the strong coupling regime. These dispersion relations are well reproduced consid-

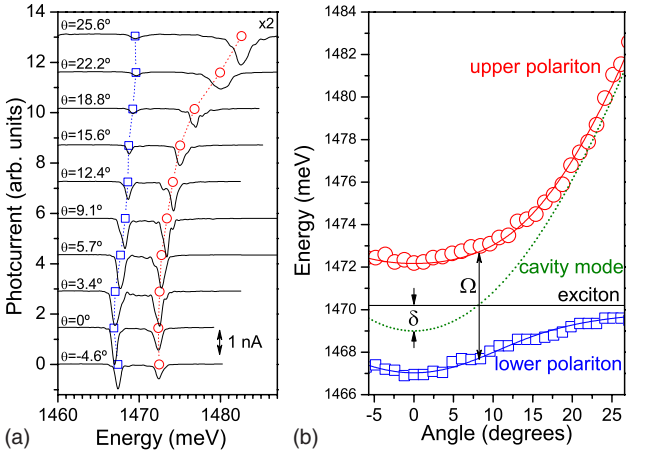

FIG. 2. (Color online) (a) Photocurrent spectra measured for various detection angles. $T=10$ K and the applied voltage is $V=1.3$ V at the limit for reverse polarization. (b) Symbols: energy of the photocurrent peaks as a function of the excitation angle. Lines: calculated energy of the uncoupled cavity mode and exciton line and of the upper and lower polariton branches using a Rabi splitting=5 meV and $\delta=-1$ meV.

ering the radiative coupling between each exciton of given $k_{\parallel}$ and energy E_x and the photon mode of same $k_{\parallel}$ and energy $E_c=\frac{\hbar c}{n}\sqrt{\left(\frac{2\pi}{L_c}\right)^2+k_{\parallel}^2}$, where n is the effective refractive index of the cavity and L_c the cavity layer thickness. The best fit is obtained using a Rabi splitting of 5 meV and a detuning $\delta=E_c(0)-E_x(0)=-1$ meV.

These measurements demonstrate that the exciton photon strong coupling regime can be achieved in a GaAs based vertical cavity with doped Bragg mirrors. Nevertheless, they do not imply the ability to electrically inject polaritons. When the diode is driven by a forward current, the strong coupling regime could, for example, be screened by the electric field induced by charge accumulation.

To test the polariton emission properties of our sample, we now consider the forward bias regime where electron-hole pairs are electrically injected into the photodiode undoped region. Figure 3(a) shows an electroluminescence spectrum measured under normal incidence for an applied bias $V=2.5$ V. Emission peaks are exactly at the same energy as the photocurrent dips measured at the same point under normal incidence. This shows that Stark shift is negligible in the considered bias conditions.[20] The emission linewidths are 0.9 and 0.6 meV for the upper and lower polariton branches emphasizing the good optical quality of this doped microcavity sample. Evidence of the strong coupling regime is obtained by monitoring the electroluminescence spectra as a function of the emission angle. Figure 3(b) summarizes the emission spectra measured under moderate injection conditions (current intensity $I=1$ mA, which corresponds to a current density $j\simeq 0.01$ A/cm^2, assuming uniform electrical injection). Both polariton branches are clearly evidenced with the characteristic s-shape of the lower branch. To estimate the carrier density, we assume that all injected carriers are trapped into the quantum well. This hypothesis is supported by the absence of GaAs emission and by the linear dependence of the total electroluminescence intensity with current

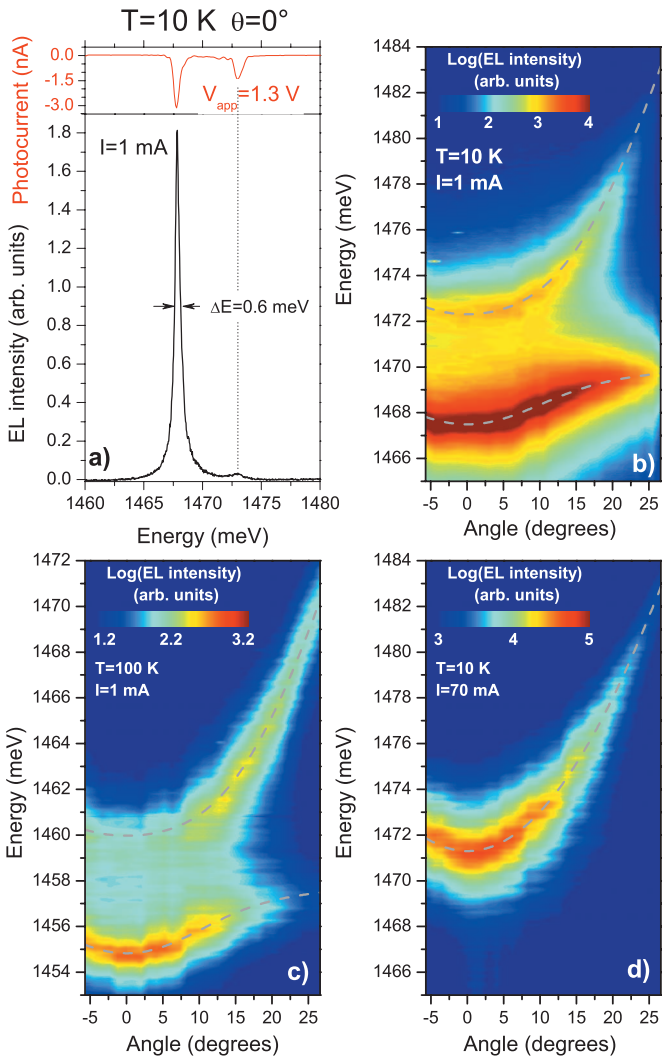

FIG. 3. (Color) (a) Photocurrent spectrum measured under normal incidence of the exciting laser beam for $V=1.3$ V, and electroluminescence spectrum measured under normal incidence for $I=1$ mA. (b)–(d) Electroluminescence spectra measured as a function of the detection angle for (b) $I=1$ mA and $T=10$ K, (c) $I=1$ mA and $T=100$, and (d) $I=70$ mA and $T=10$ K. In (b) and (c), the dotted lines correspond to the calculated upper and lower polariton branches using $\Omega=5$ meV and the intensities are in logscale. In (d), the dotted line corresponds to the cavity mode dispersion.

intensity, indicating that nonradiative processes can be neglected. As a result, the total electron-hole pair density n can be directly deduced from the current density, the same way as it is usually deduced from the excitation power under optical pumping. Thus, $n=j\tau/e$, where e is the electron charge and τ the averaged recombination time (typically 200–400 ps in such samples[21]). For $I=1$ mA, the estimated value of the polariton density is of the order of $n\simeq(1-3)\times10^9$ cm^{-2}. Figure 3(d) summarizes the measured electroluminescence spectra at a higher current intensity ($I=70$ mA and $j\simeq0.78$ A/cm^2): In this case, a single emission line is observed in the electroluminescence spectra with the characteristic dispersion relation of the bare cavity mode. The estimated carrier density for $I=70$ mA lies around 7×10^{10} cm^{-2} and is beyond the Mott density (typically of the order of some 10^{10} cm^{-2}.)[22] In this density regime, excitons are bleached by the screening of the Coulomb interaction and phase space filling: the optical properties are therefore dominated by the recombination of uncorrelated electron-hole pairs. This continuum of unbound electron-hole pairs is in the weak coupling regime with the cavity mode, and the emission is simply filtered by the cavity mode. Thus, Figs. 3(b) and 3(d) illustrate the transition from the strong coupling to the weak coupling regime when increasing the density of electrically injected electrons and holes.

To investigate the operability range of the present polariton device, electroluminescence measurements were performed at different temperatures. The detuning between the exciton and the cavity mode increases with temperature. The present wafer exhibits detuning close to zero only up to 100 K. This has determined the upper limit of the operating temperature that could be tested in the present sample. As shown in Fig. 3(c), the strong coupling regime still persists at 100 K: both polariton branches are observed with a significant broadening of the emission lines (0.8 and 1.5 meV for the lower and upper branches) induced by increased polariton-phonon interaction.

To summarize, we report the clear demonstration of electrically driven polariton emission in a semiconductor microcavity. This opens the way toward new sample designs suitable for the realization of electrically pumped polariton lasers. Note that in the present work, the excitation is nonresonant so that the relaxation bottleneck[23] limits the occupation of the ground state. To circumvent this problem and reach quantum degeneracy under electrical injection, cavities with reduced dimensionality can be considered.[14,15] Another approach could be the use of resonant tunneling to directly inject polaritons into the lower branch states. Finally, strong technological developments[24] could possibly allow the same approach in the GaN system[13,25] to reach room temperature polariton lasing.

This work was funded by the European project "Clermont 2" (MRTN-CT-2003-503677), by "C'nano Ile de France" and "Conseil Général de l'Essonne."

*jacqueline.bloch@lpn.cnrs.fr

[1] E. M. Purcell, Phys. Rev. **69**, 681 (1946).
[2] R. J. Thompson, G. Rempe, and H. J. Kimble, Phys. Rev. Lett. **68**, 1132 (1992).
[3] A. Wallraff, D. I. Schuster, A. Blais, L. Frunzio, R. S. Huang, J. Majer, S. Kumar, S. M. Girvin, and R. J. Schoelkopf, Nature (London) **431**, 162 (2004).
[4] C. Weisbuch, M. Nishioka, A. Ishikawa, and Y. Arakawa, Phys.

Rev. Lett. **69**, 3314 (1992).
[5] D. G. Lidzey, D. D. C. Bradley, M. S. Skolnick, T. Virgili, S. Walker, and D. M. Whittaker, Nature (London) **395**, 53 (1998).
[6] D. Dini, R. Köhler, Alessandro Tredicucci, Giorgio Biasiol, and Lucia Sorba, Phys. Rev. Lett. **90**, 116401 (2003).
[7] T. Yoshie, A. Scherer, J. Hendrickson, G. Khitrova, H. M. Gibbs, G. Rupper, C. Ell, O. B. Shchekin, and D. G. Deppe, Nature (London) **432**, 200 (2004).
[8] J. P. Reithmaier, G. Sek, A. Loffler, C. Hofmann, S. Kuhn, S. Reitzenstein, L. V. Keldysh, V. D. Kulakovskii, T. L. Reinecke, and A. Forchel, Nature (London) **432**, 197 (2004).
[9] E. Peter, P. Senellart, D. Martrou, A. Lemaître, J. Hours, J. M. Gérard, and J. Bloch, Phys. Rev. Lett. **95**, 067401 (2005).
[10] R. Houdré, C. Weisbuch, R. P. Stanley, U. Oesterle, P. Pellandini, and M. Ilegems, Phys. Rev. Lett. **73**, 2043 (1994).
[11] H. Deng, G. Weihs, C. Santori, J. Bloch, and Y. Yamamoto, Science **298**, 199 (2002).
[12] J. Kasprzak, M. Richard, S. Kundermann, A. Baas, P. Jeambrun, J. M. J. Keeling, F. M. Marchetti, M. H. Szymanska, R. Andre, J. L. Staehli, V. Savona, P. B. Littlewood, B. Deveaud, and Le Si Dang, Nature (London) **443**, 409 (2006).
[13] S. Christopoulos *et al.*, Phys. Rev. Lett. **98**, 126405 (2007).
[14] R. Balili, V. Hartwell, D. Snoke, L. Pfeiffer, and K. West, Science **307**, 1007 (2007).
[15] D. Bajoni, P. Senellart, E. Wertz, I. Sagnes, A. Miard, A. Lemaître, and J. Bloch, Phys. Rev. Lett. **100**, 047401 (2008).
[16] M. Romanelli, C. Leyder, J. Ph. Karr, E. Giacobino, and A. Bramati, Phys. Rev. Lett. **98**, 106401 (2007).
[17] C. Leyder, M. Romanelli, J. Ph. Karr, E. Giacobino, T. C. H. Liew, M. M. Glazov, A. V. Kavokin, G. Malpuech, and A. Bramati, Nat. Mater. **3**, 628 (2007).
[18] J. R. Tischler, M. S. Bradley, V. Bulovic, J. H. Song, and A. Nurmikko, Phys. Rev. Lett. **95**, 036401 (2005).
[19] L. Sapienza, A. Vasanelli, R. Colombelli, C. Ciuti, Y. Chassagneux, C. Manquest, U. Gennser, and Carlo Sirtori, Phys. Rev. Lett. (to be published).
[20] T. A. Fisher, A. M. Afshar, D. M. Whittaker, M. S. Skolnick, J. S. Roberts, G. Hill, and M. A. Pate, Phys. Rev. B **51**, 2600 (1995).
[21] B. Sermage, S. Long, I. Abram, J. Y. Marzin, J. Bloch, R. Planel, and V. Thierry-Mieg, Phys. Rev. B **53**, 16516 (1996).
[22] L. Kappei, J. Szczytko, F. Morier-Genoud, and B. Deveaud, Phys. Rev. Lett. **94**, 147403 (2005), and references therein.
[23] F. Tassone, C. Piermarocchi, V. Savona, A. Quattropani, and P. Schwendimann, Phys. Rev. B **56**, 7554 (1997).
[24] A. Castiglia, D. Simeonov, H. J. Buehlmann, J.-F. Carlin, E. Feltin, J. Dorsaz, R. Butté, and N. Grandjean, Appl. Phys. Lett. **90**, 033514 (2007).
[25] F. Semond, I. R. Sellers, F. Natali, D. Bryne, M. Leroux, J. Massies, N. Ollier, J. Leymarie, P. Disseix, and A. Vasson, Appl. Phys. Lett. **87**, 021102 (2005).